Proceedings of ASME Turbo Expo 2011
GT2011
June 6-10, 2011, Vancouver, British Columbia, Canada

GT2011-46834

ANNULAR CASCADE FOR RADIAL COMPRESSOR DEVELOPMENT

Christian Aalburg
GE Global Research
Garching, Germany

Ismail Sezal
GE Global Research
Garching, Germany

Christian Haigermoser
GE Global Research
Garching, Germany

Alexander Simpson
GE Global Research
Garching, Germany

Vittorio Michelassi
GE Oil&Gas
Florence, Italy

Giuseppe Sassanelli
GE Oil&Gas
Florence, Italy

ABSTRACT

A full-annulus cascade for radial compressor stator development has been designed and commissioned. The cascade has been developed for the rapid screening of novel stator concepts to facilitate risk mitigation in the early design phase and the validation/calibration of numerical predictions. The rig consists of two main parts. The first part is comprised of an exchangeable set of stationary preswirl vanes that have been designed to mimic discrete points on the operating characteristic of the impeller. The second part consists of a diffuser, bend and return channel with return channel vanes that can also be quickly exchanged. All exchangeable parts are manufactured by rapid prototyping, allowing rapid turnaround times from aerodynamic design to full validation. This is achieved at a significantly lower cost than that of a full rotating test.

This investigation summarizes the experimental results and numerical predictions of two test rigs that were designed to study the effect of diffusion ratio, i.e. the ratio of the maximum outer diameter at the top of the bend to the exit of the impeller, on stator performance. To further investigate the sensitivity of the aerodynamic performance to different flow conditions, metal gauzes were positioned immediately downstream of the trailing edges of the preswirl vanes. This allowed the modification of angle and pressure distributions in the diffuser and bend as well as the setting of different turbulence conditions (intensity and length scale) in the downstream sections.

NOMENCLATURE

Symbols

Cp	Pressure recovery coefficient $(P_s-P_{s,ref})/(P_{0,ref}-P_{s,ref})$ [-]
L	Length
P	Pressure [Pa]
R	Radius
Solidity	$(R_{le}-R_{te})$ #vanes / $(2\pi R_{te})$
Yaw	Angle measured relative to the radial coordinate
Y^+	Dimensionless wall distance [-]
ζ	Loss coefficient $(P_{0,Inlet}-P_{0,Exit})/(P_{dyn,Inlet})$ [-]

Subscripts

ax	Axial
b	Bore
dyn	Dynamic quantity (stagnation – static)
ie	Impeller exit
le	Vane leading edge
max	Maximum at top of the bend
s	Static quantity
te	Vane trailing edge
0	Stagnation quantity
1	Stage inlet plane
2	Impeller exit plane
3	Diffuser exit plane
4	Stage exit plane

INTRODUCTION

Industrial radial compressors are typically multistage machines. Each stage consists of a rotating centrifugal impeller and a stationary stator consisting of a vaneless or vaned diffuser, bend and return channel with return channel vane.

The performance of the stator parts in terms of pressure loss and operability (the range between choke and stall) has a significant influence on the overall stage characteristics. It is not unusual for 5-10 points of compressor efficiency to be lost in the stator section. Further, the radial dimension of the compressor and thereby the manufacturing cost of the casing are proportional to the length of the diffuser.

Improving existing stator technologies has thus been the focus of a number of recent development efforts on radial compressors. Examples include [1] and [2] in which flow control was applied to the suction side of the return channel vane for increased operability. In [3], the return channel vane was extended upstream across the 180° bend for improved efficiency. Finally, in [4] advanced, three-dimensional return channel designs were introduced that allowed reducing the outer diameter without compromising performance.

One challenge with the development of new stator designs is the validation and testing. Testing new designs in a full rotating test environment is a time-consuming and expensive process that requires the dedication of significant resources. The step from CFD analysis straight to a rotating test also carries considerable risk. This is particularly important when designs fall outside the known design space.

In the field of axial turbomachinery linear cascades have been used as an additional step between the CFD analysis and a rotating test [5]. Cascade testing provides an inexpensive, simplified environment in which high fidelity measurements can be taken and quickly fed back to the design/development loop. However, it should be noted that the cascade approach fails to capture some important flow phenomena, such as unsteadiness. Hence it cannot be used as a replacement for a final validation test on a rotating compressor test bed.

The need for an inexpensive test rig for the screening of new stator concepts for radial compressors led to the development of a full-annulus cascade. The cascade was designed with a stationary sets of preswirl vanes in place of the rotating impeller. The vanes were shaped to provide similar flow conditions at the entrance to the diffuser at discrete points on the operating characteristic (except for the unsteadiness). The design objectives can be summarized as follows:

1. Compatibility with a range of blow-down test facilities for low cost operation and design.
2. Four week turn-around times from design to completed test.
3. No geometrical scaling to facilitate one-to-one comparison with rotating test conditions.
4. Variable operating conditions to allow testing over the full range of flow coefficients (choke to surge).
5. Employment of a range of high-resolution measurement techniques at locations compatible with rotating tests for data matching and CFD calibration.
6. The ability to adjust turbulence conditions in order to facilitate investigations of turbulence.

This paper begins with a description of the role the test rig plays in the overall stage development strategy. Following this discussion the details of the test rig, its instrumentation and supporting infrastructure will be described. The discussion will then consider the commissioning of the test rig including validation measurements and a detailed analysis of the measurement accuracies. Finally, test results for the performance of two stators with different diffusion ratios will be presented along with a study on the impact of metal gauzes on flow distributions and turbulence conditions in the diffuser and bend.

ROLE IN OVERALL STAGE DEVELOPMENT STRATEGY

The objective of the full-annulus radial cascade is to provide a fast and cost efficient means for early risk retirement in the development process of new technologies for radial compressors. More precisely, the full-annulus cascade is aimed at closing the gap between numerical based design and analysis of radial compressor stages and the testing of these designs in a full rotating test environment. As such it provides for the validation of predictions of aerodynamic performance and detailed flow conditions of the stator components at various operating conditions and provides an effective means of screening new concepts.

Since the test environment is steady, i.e. without any rotating parts, the radial cascade has a number of advantages over a rotating test. Firstly, the design and manufacturing of all required components can be achieved at only a fraction of the cost of a rotating test. Secondly, it facilitates the use of rapid prototyping which, combined with a flexible and modular test rig approach, allows turnaround times of less than four weeks between the design of a new stator vane and the validation of its performance. And thirdly, the steady nature of the test provides a relatively simple environment for the implementation of optical flow measurements (LDA or PIV) or hot-wire anemometry for the systematic calibration of analytical and numerical models.

The full-annulus radial cascade described in this paper is currently being used as part of an ongoing development strategy that is aimed at reducing the outer diameter of centrifugal compressors and increasing the efficiency. It is a natural extension of the 90° sector test rig that had been previously developed [6]. The advantages of a full-annulus vs. a 90° sector test rig are improved periodicity of the flow and

increased operability in terms of the range of possible flow angles delivered by the preswirl section. Both of which are limited in the 90° sector test rig by the presence of fixed walls along the sides of the test rig. On the other hand, a 90° sector test rig requires only one fourth of the massflow which may not always be available in the full amount.

In order to reduce outer diameters, the diffusion ratio, which is defined as the ratio of the outer radius at the top of the bend to the impeller exit radius, has been reduced in two steps over current designs: from 1.94 down to 1.84 and 1.60, corresponding to a 5% and 18% reduction over the baseline design, respectively. Additionally, the axial span (L_{ax}) was reduced by 20% and the ratio of impeller bore/exit diameter (R_b/R_{ie}) increased from 0.3 to 0.4. A schematic of the three return channels is shown in Fig. 1 and a summary of the corresponding stage parameters is given in Table 1. Return channel vane parameters such as leading and trailing edge angles and solidity were reasonably constant between the three flow paths. The second objective, i.e. an increase in efficiency, is pursued with new stator concepts that are being validated and compared against a conventional baseline design.

Based on these test results the most successful configurations in terms of diffusion ratio and stator concept will be selected for final validation on a rotating test.

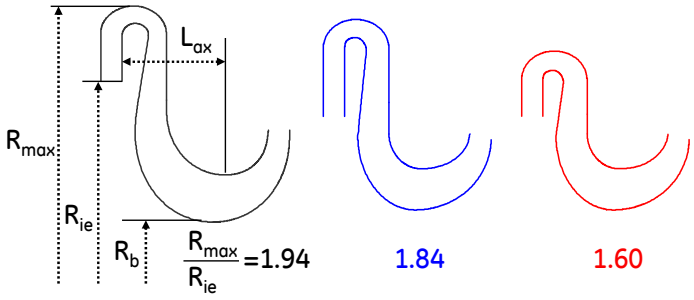

Figure 1: Schematic of the flow path of three return channels. The number under each schematic corresponds to diffusion ratio (the radius ratio of top of bend to impeller exit).

Diffusion ratio (radius ratio of top of bend/impeller exit) [-]	1.94	1.84	1.60
Design flow coefficient [-]	0.1273	0.1273	0.1273
Imepeller/preswirler exit diameter [mm]	340	340	340
No. of impeller/preswirl blades/vanes	14	14	14
No. of return channel vanes	16	14	18
Solidity [-]	3.2	3.2	3.1

Table 1: Summary of stage parameters

THE FULL-ANNULUS CASCADE

This section will present a description of the test rig and the supporting infrastructure.

The test rig was designed as a full-annulus of a radial compressor stage in full scale consisting of a non-rotating impeller ("Preswirler") followed by diffuser, bend and return channel with return channel vane. Figure 2 shows a schematic of the test rig. The rotating impeller was replaced by four exchangeable sets of stationary preswirl vanes that were shaped such that they provided spanwise exit flow profiles similar to those of the rotating impeller at discrete points of the operating characteristic. Vanes, hub and shroud were integrated into a single part in order to avoid leakage between the vanes and the endwalls as a result of manufacturing tolerances. The stator components, i.e. diffuser, bend, return channel and return channel vane, were combined into one part, also integrating the vanes with the endwalls in order to avoid leakage.

Both the preswirl and the stator parts were divided circumferentially into several segments (typically 4-5). The full-annulus vane sets were obtained by mounting the segments onto aluminum plates which were then inserted into the aluminum casing (see Fig. 2). The casing was split into two halves: one for the inlet and one for the outlet section. This allowed pre-assembly of different geometries and rapid exchange of preswirl and stator geometries during testing. It was possible to leave the majority of the instrumentation, such as traversing probes, in place during the exchange of the geometries. However, pressure tubings for endwall and vane surface pressure tappings had to be reconnected. All parts except for the mounting plates and the casing were manufactured by rapid prototyping.

The test section was integrated in a blow down test facility shown in Fig. 3. The airflow is provided by a blower delivering in excess of 8 kg/s at up to 1.6 bar absolute pressure. A heat exchanger downstream of the blower maintains air temperatures below 80°C. Valves 1 and 2 are primarily used to set the mass flow through the test section while valve 3 mainly regulates the pressure in the test section. Figure 4 shows photographs of the cascade segments and the overall test facility.

Several steps were taken to ensure that the test section receives a carefully controlled inlet flow. Upstream of the test section and downstream of the 180° bend shown in Fig. 3, a flow conditioning section including honeycomb, fine gauze and an area contraction are positioned. Immediately downstream of the contraction a second exchangeable gauze allows setting turbulence conditions at the inlet to the test section. The setup used for the present investigation yielded a turbulence intensity of 2% at the inlet to the test section. A diffuser and a 4m straight pipe section are connected the exit of the test section with the third throttle valve.

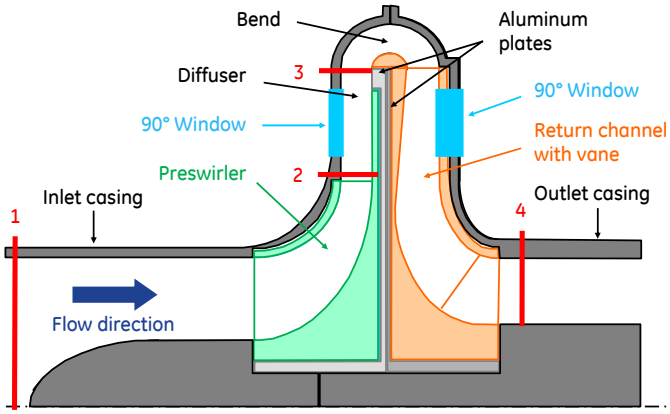

Figure 2: Schematic of full-annulus radial cascade.

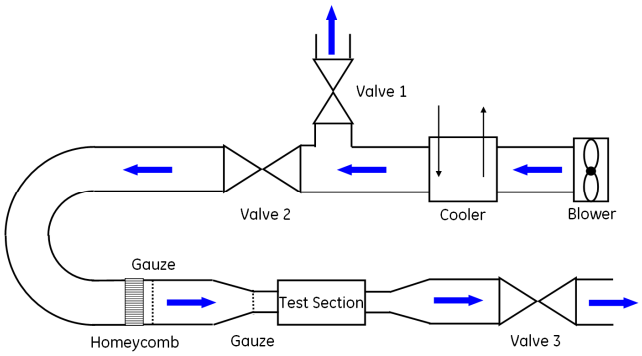

Figure 3: Schematic of overall test facility.

Figure 4: Top: Photographs of the cascade segments. From left to right: preswirl section, return channel segment and assembled return channel section. Bottom: Photographs of test section (left) and overall test facility (right).

The test rig is equipped with a range of instrumentation at the measurement sections labelled 1-4 shown in Fig. 2. The measurement section 2, 3 and 4 coincide with the locations used in corresponding rotating tests. Mass flow measurements were conducted with a mass flow meter (vortex type) downstream of valve 2 (see Fig. 3) and by traversing Kiel and 5-hole probes at section 1.

The instrumentation at section 1 consists of 4 circumferentially evenly distributed static pressure tappings at the pipe wall and spanwise traverses of a 5-hole probe (vertical traverse) and a Kiel probe (horizontal traverse). The 5-hole probe was replaced by a single wire hotwire probe for the characterization of turbulence conditions.

Measurement section 2 is positioned immediately downstream of the preswirl vanes and represents the inlet to the diffuser. The instrumentation at section 2 included a 5-hole probe that was traversed in both the spanwise and circumferential directions across up to three preswirl vane pitches. The typical resolution for this area traverse was 17×17 points per pitch. This probe was replaced by a hotwire probe for turbulence measurements (intensity, length scale). Additionally, three Kiel probes (for redundancy of stagnation pressure measurements) and three temperature probes (j-type thermocouples) were positioned at fixed locations in different pitches. Static pressures were measured at six circumferential locations each at the hub and at the shroud wall and distributed over several pitches.

Measurement section 3 is located at the diffuser exit and immediately upstream of the 180° bend. The instrumentation was identical to section 2, except that in this case temperatures were not measured.

The stage exit is represented by measurement section 4. This section was instrumented with a 5-hole probe that was traversed in both the spanwise and circumferential direction across three return channel vane pitches. The typical measurement resolution was 17×17 points per pitch. This probe was replaced by a hotwire probe for turbulence measurements. Further, two rakes with seven Kiel probes (for redundancy of stagnation pressure measurements) and two rakes with seven thermocouples were installed in fixed circumferential position. Finally, hub and shroud wall were equipped each with five static pressure tappings distributed over several pitches.

Static pressure tappings were also included on the adjacent vane surfaces of two flow channels in the return channel section. The two vane suction sides were equipped with five tappings along the chord each at 20%, 50% and 80% span (15 tappings in total per vane suction side) and the two vane pressure sides had each five tappings along the chord at 50% span.

Provisions for more detailed measurements of the flow field using PIV or LDA techniques were provided by two windows. These provided optical access to a 90° sector of the diffuser and the return channel in the proximity of the bend (see Fig. 2).

A total of four sets of preswirl vanes were used to simulate four different operating conditions along the compressor characteristic. The preswirlers had been designed to match flow conditions in terms of spanwise profiles of yaw angle and stagnation pressure that had been measured downstream of an existing impeller (section 2) during a rotating test. Details of the numerical design can be found under the section titled "Numerical Methods". In addition to the flow profiles, the full-annulus cascade was operated such that volume flows and temperatures at section 2 were close to those encountered at the impeller exit of the corresponding rotating test in order to match Mach numbers (volume flows were typically within 5%, temperatures typically within 10°C).

The magnitude of the stator losses are indicated by the loss coefficient between sections 2 and 4 as follows:

$$\zeta = \frac{P_{0,2} - P_{0,4}}{P_{0,2} - P_{s,2}} \quad (1)$$

Sectional area averages were used to calculate the stagnation and static pressures at sections 2 and 4. An evaluation of the associated measurement uncertainties is presented in the next section.

MEASUREMENT ACCURACIES

This section summarizes measurement uncertainties and their impact on the measurement accuracy of the stator loss coefficient. Figure 5 illustrates the error sources and their impact on the sectional averages of stagnation and static pressure. For each error source the corresponding uncertainties of the sectional pressure averages were introduced in a Monte Carlo simulation of the stator loss coefficient. The resulting uncertainties of the loss coefficient are given below for 95% confidence.

Starting from the real flow property Q, e.g. stagnation pressure, the calibration uncertainty of the sensor, e.g. the 5-hole probe, and the measurement uncertainty, e.g. of the pressure sensor, cause an error on the measured quantity. For the present test campaign, the calibration error on total and static pressures measured with the 5-hole probe was ±0.02% according to the certificates provided by the probe manufacturer. Pressure signals were acquired with Scanivalve differential pressure sensor arrays DSA 3018 with acquisition ranges of 1 PSID, 2.5 PSID and 5 PSID. The associated measurement uncertainties were ±0,12%, ±0,12% and ±0,05% of the full range, respectively. This yields a calibration and measurement error of 2.4% each on the loss coefficient.

The conversion of point measurements to sectional averages is affected by three sources of uncertainty: resolution error, a drift of inlet conditions and pitch-to-pitch variation. The resolution error was determined by coarsening the resolution of an existing measurement. This was done by discarding measurement points such that the test matrix was progressively reduced from 17×17 down to 9×9, 5×5 and 3×3 points per pitch. Richardson extrapolation [7] towards infinite resolution revealed that the measurement resolution of 17×17 points per pitch yielded sectional averages of pressure that were within 0.01% and 0.05% of the expected average at infinite resolution at sections 2 and 4, respectively. The corresponding error on the stator loss coefficient was determined to be 4.6%.

Traversing over almost 1,000 points (3 pitches each of 17×17 points) is a time consuming process. The typical test campaign took approximately four hours per operating point: one hour for the stabilization of the test facility followed by three hours of data acquisition. Despite the warm-up period, a certain drift of inlet conditions could not be avoided. The change in inlet pressure was typically on the order of 100 Pa over the data acquisition period. Since the drift largely is effectively nulled in the computing of the loss coefficient, the associated error was determined to be of the order of 0.1%.

The largest source of error for the loss coefficient was found to be the pitch-to-pitch variation of the sectional averages. After subtracting effects of drift (traversing proceeded in the spanwise direction first), manufacturing tolerances of the preswirl and return channel vanes as well as clocking effects between the preswirl vanes and the return channel vanes yielded uncertainties of 7.9% for the stator loss coefficient.

Summation of the variances for each error source yielded an overall uncertainty of 11.0% for 95% confidence on the stator loss coefficient. This was found to be reasonable and sufficient for the purposes of this screening test rig.

The uncertainties of measurements of stagnation temperature with j-type thermocouples were ±1°C. Uncertainties in the measured flow angles were of the order of ±0.5°.

Finally, unsteady velocities were acquired at sections 0, 2, 3 and 4 using a two channel TSI anemometer together with two L-shaped Dantec 55P14 single wire hot wire probes. The probes were calibrated by placing them at section 0 together with a 5-hole probe. Thereby, calibration was performed very close to the temperature and pressure encountered during the measurements at the different sections. Remaining differences in temperature between the calibration and the measurement were corrected using Bearman's correction [8] of the acquired voltage. Differences in pressure were corrected by scaling the obtained velocity with the ratio of the static pressure from calibration and measurement. The hotwire probes were traversed in the same manner as the 5-hole probes at the respective sections, except that angular traversing was applied in order to rotate the hotwire probes into the direction of the flow such that the angle between the hotwire and the flow was perpendicular at each measurement point. A comparison of the velocity fields measured with the 5-hole probes and the hotwire probes showed that differences between the two measurements were less than 5%.

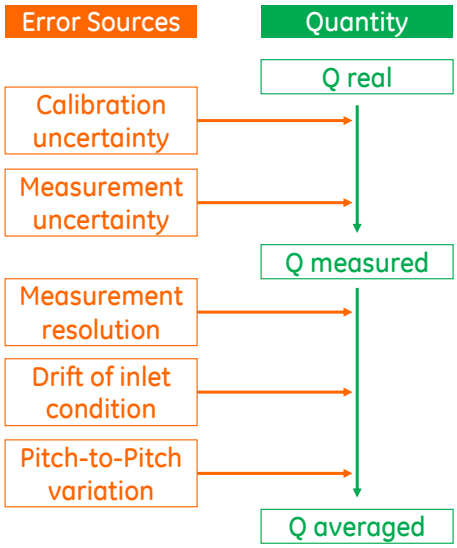

Figure 5: Error sources impacting the accuracy of averaged quantities reported in this study.

NUMERICAL METHODS

The numerical computations presented in this paper were performed using ANSYS CFX-12. The geometries for different sets of preswirl vanes and return channel vanes were created using AxCent from Concepts NREC. The geometries were discretized using CFX-TurboGrid with an O-H grid topology. In all cases perfect symmetry between blade passages was assumed, therefore only one flow channel was modeled with matching periodic boundary conditions along the sides.

During the design of the preswirl vanes, the computational domain included the preswirl section and the return channel section with a mixing plane between the two sections. Uniform stagnation pressures and temperatures were prescribed at the inlet whereas mass flow was fixed at the outlet (see Fig. 2).

For the comparison with measurements the computational domain included only the return channel. The measured spanwise profiles of stagnation pressure and temperature as well as yaw and pitch angles were prescribed at the inlet (measurement section 2) and the corresponding mass flow of the test was prescribed at the outlet (see Fig. 2).

The computational grid in the preswirl section consisted of 1.5 million cells per blade passage and the grid resolution at surfaces in terms of dimensionless wall distance was of the order of $y^+ \approx 1$, allowing for wall integration. The computational grid of the return channel section consisted of between 1.2-1.5 million cells per passage, depending on the diffusion ratio. The dimensionless wall distance was of the order of $y^+ \approx 40$ and automatic wall functions were used for the calculation of shear stresses. The k-ω turbulence model was used for all the results presented in this paper. Calculations were run to steady-state and typical computation times were three hours with eight processors on a HP Blade cluster.

VALIDATION OF THE CONCEPT

The following section summarizes the commissioning and validation of the new test rig. This includes the validation of uniform inlet conditions at the inlet to the test section, a comparison of the flow profiles delivered by the preswirl vanes to those seen in the rotating machine, and the periodicity of two adjacent return channel flow channels.

Figure 6 illustrates yaw and pitch angles as a function of span as measured by the 5-hole probe at the inlet to the test section (across the inlet pipe, section 1 in Fig. 2). The results show uniform flow throughout the pipe with no residual vorticity from upstream bends (Fig. 2) in the piping. The increase in pitch angle close to the wall is due to the presence of a minor degree of leakage around the stem of the probe. The general offset of approx. 2° for each angle is caused by misalignment (section 1 did not have a reference point as opposed to all downstream sections and thus was aligned by visual inspection).

Figure 7 shows measurements and predictions of the spanwise profile of circumferentially area averaged yaw angle at the inlet to the diffuser (section 2) in addition to measurements of a corresponding test with a rotating impeller. The qualitative agreement between the CFD target profile and the achieved result is reasonable, however, the average yaw angle delivered by the preswirl vanes is slightly smaller than the target from the rotating test point. This is likely to be attributable to significant unguided turning near the trailing edge. Also, the flow weakness close to the shroud revealed by the large yaw angles associated with reduced stagnation pressure and velocity is more pronounced in the full-annulus cascade than in the rotating test. When moving downstream to section 3, i.e. the diffuser exit, the deviations between the target and the achieved profiles were, however, significantly reduced with the exception of the shift in the average angle. As a consequence of this shift, this set of preswirl vanes represented an operating point of 98% of the design flow coefficient instead of 96% originally targeted. A similar shift was observed also for the other sets of preswirl vanes and had no consequence on the value or validity of the results obtained with the present radial cascade.

Figure 8 illustrates contour plots of measured (top) and predicted (bottom) stagnation pressure at the inlet to the diffuser (section 2). Both results were post processed in the same manner, i.e. by extracting data from the CFD prediction in correspondence with the measurement probe locations and by normalizing each plot with its sectional average. The plot area of Fig. 8 covers 2.5 pitches in the circumferential direction and the spanwise length that was accessible to the 5-hole probe (between 8-92% span). The agreement between measurements and predictions is found to be reasonable. Pitchwise location, width and magnitude of the wakes of the upstream preswirl vanes are captured well by the CFD. The weak core of the wake is predicted slightly further away from the hub wall as compared with the measurements and in proximity to the shroud the measured wake reveals a stronger interaction with

the sidewall boundary layer than in the predictions. Pitch-to-pitch variations in the measurements are also visible in Fig. 8, which are largely attributable to manufacturing tolerances.

Figure 9 illustrates measurements and predictions of the static pressure distribution of the return channel vane surfaces of two adjacent flow channels at mid span. The operating point corresponds to 98% design flow coefficient and the diffusion ratio was 1.60. The results are normalized by static and stagnation pressures at the inlet to the diffuser (section 2 of Fig. 2). The agreement between numerical predictions, i.e. the design intent, and the achieved pressure distribution is good. Furthermore, in spite of the different vane count for this small diffusion ratio (14 preswirl vanes vs. 18 return channel vanes) the measurements exhibit minimal variation between flow channels. This suggests that the pitch-to-pitch variation observed in Fig. 8 does not play a major role in the aero-response of the downstream channel.

In summary, the full annular cascade concept delivers flow conditions at the inlet to the diffuser that are reasonably close to the corresponding impeller exit conditions with the exception of the unsteadiness. The flow conditions were further verified at the exit of the diffuser and in terms of the static pressure distributions on the return channel vane surfaces and were found to be in good agreement with the design intent. The next section will summarize the results of a test campaign that was carried out in the annular cascade with the aim of investigating the effect of diffusion ratio on the performance of the return channel of centrifugal compressors.

RESULTS

As mentioned previously, the full-annulus radial cascade that has been designed and developed in the current investigation is being used as part of an ongoing development strategy that is aimed at reducing the outer diameter and at further increasing the efficiency of current centrifugal compressor stages.

In the following, the performance of two stators as measured and predicted in the present cascade will be compared against a baseline design for which test data from a full rotating test is available. All three geometries share similar designs for diffuser, bend and return channel. The main difference is the diffusion ratio, which was reduced from the baseline design of 1.94 down to 1.84 and 1.60, respectively (see Fig. 1). The tests in the full-annulus cascade were carried out at four different flow coefficients, i.e. at 70%, 86%, 98% and 145% of the design flow coefficient. Each operating point corresponds to a different preswirler design.

Figure 10 compares the measured and computed normalized total pressure field at section 4, i.e. at the stage exit. The results are shown for the geometry with a diffusion ratio of 1.84 at 98% of the design flow coefficient. The numerical predictions show a pattern that is quite similar to the measurements both qualitatively and quantitatively. This trend is particularly notable nearing the vicinity of the shroud. The wakes of the three return channel vanes are pronounced in both plots. However, details of the wake pattern differ somewhat, mostly on account of larger tangential gradients predicted by CFD. Similar agreement was found for other flow quantities. The reasonable periodicity observed in the measurements of Fig. 10 (top plot) is another indicator that the clocking effect of the stationary preswirl vanes was not significant for the present test conditions.

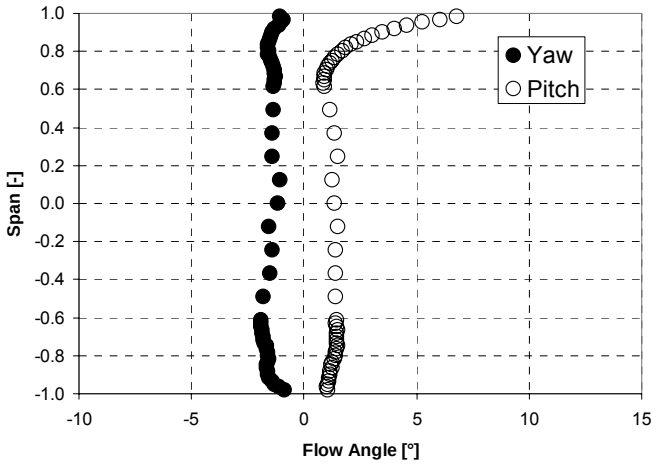

Figure 6: Measured yaw and pitch angles at the inlet to the test section (section 1) as a function of span (across the inlet pipe).

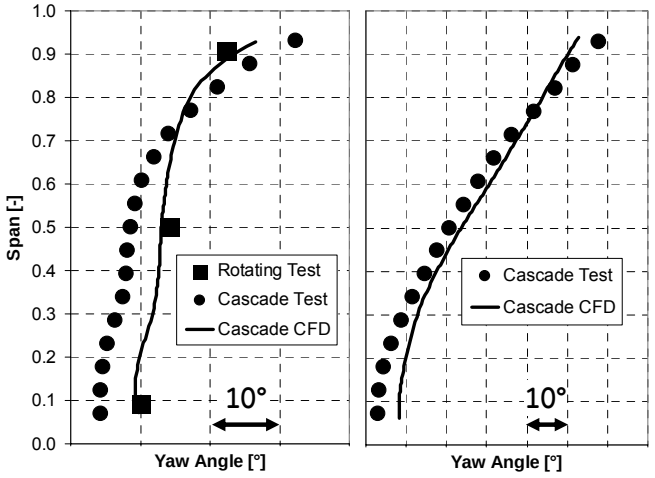

Figure 7: Circumferentially area averaged yaw angle as a function of span at the inlet to the diffuser (section 2: left side) and at the exit of the diffuser (section 3: right side) at 98% design flow coefficient. Shown are measurements and predictions of the present test rig and measurements from a corresponding rotating test.

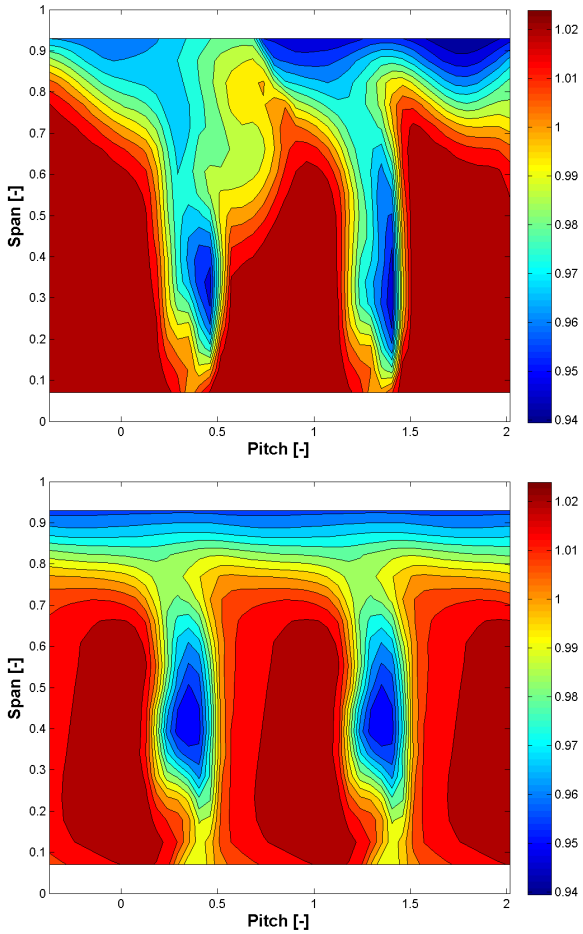

Figure 8: Contour plots of measured (top) and predicted (bottom) stagnation pressure at the inlet to the diffuser (section 2) at 98% design flow coefficient. Pressures are normalized with the respective sectional average.

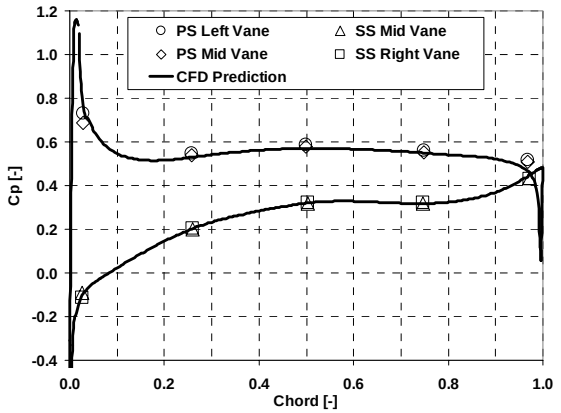

Figure 9: Measurements and predictions of static pressure distribution of return channel vane surfaces of two adjacent flow channels at mid span and at 98% design flow coefficient. Pressures are normalized with static and stagnation pressures at section 2.

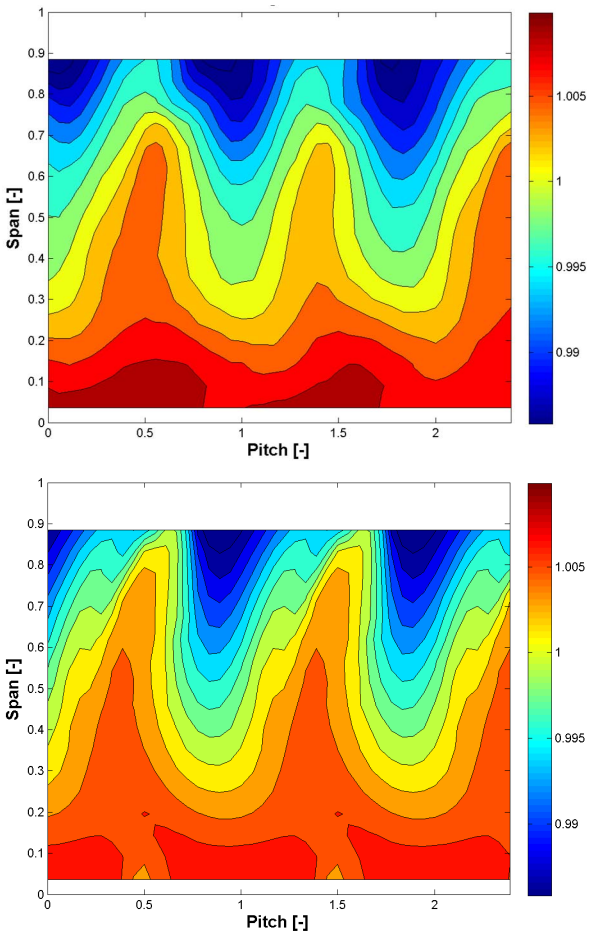

Figure 10: Contour plots of measured (top) and predicted (bottom) stagnation pressure at the stage exit (section 4) at 98% design flow coefficient. Pressures are normalized with the respective sectional average.

Figure 11 illustrates measurements and predictions of circumferentially area averaged yaw angles as a function of span at the stage exit (section 4) for the two different diffusion ratios (1.84 and 1.60) at 98% of the design flow coefficient. Both return channels show the same characteristic, i.e. minimum yaw angles near the endwalls and a maximum slightly above mid span. Overall flow turning is observed to be larger for the small diffusion ratio design. The numerical predictions closely follow the same trends and qualitative profile shapes, however, overall flow turning is generally significantly under predicted by 5-10°.

Figure 12 finally compares the performance of the two reduced radius return channel geometries against the baseline design in terms of the loss coefficient between section 2-4. Shown are measurements and predictions of the reduced radius designs at the four discrete operating points of the present cascade along with the results of a rotating test of the baseline design. The results indicate that pressure losses were significantly reduced with the new 1.84 diffusion ratio design

as compared to the baseline performance over the majority of the speedline (except near the right limit). This was achieved in spite of a reduction in diffusion ratio (from 1.94 down to 1.84) that corresponds to a 5% reduction in stage diameter. It should be noted that the measured stator loss coefficient of the baseline design exhibits an unusual decrease rather than an increase towards the right limit and thus may be unreliable at large flow coefficients. A further reduction in diffusion ratio from 1.84 down to 1.60 (18% reduction over baseline design) significantly increased the stator losses to magnitudes greater than the baseline design except near the design point.

The numerical predictions of the stator losses of Fig. 12 are generally in reasonable agreement with the measurements. In particular, the relative difference between the two diffusion ratio designs as well as trends and, at some operating points, even absolute values, are captured by the simulation. However, the overall tendency is to under predict pressure losses. This may be attributable to the circumferential averaging of the spanwise profiles that were prescribed as inlet condition for the computations. This approach neglects mixing losses associated with the circumferential gradients in the flow (see Fig. 8). The largest differences to the measurements are found near the right limit of the operating characteristic.

Cumpsty [9] refers to a degree of controversy surrounding the effect of turbulence of the inflow of axial compressors. He points to the work of Schlichting and Das [10], De Haller [11] and Wisler [12] who worked on both cascades and multistage compressors. Japikse and Baines [13] also point to a lack of knowledge about the influence of turbulence on the flow in radial vaneless diffusers. Further improvements in the accuracy of the numerical predictions are thus believed to be achievable by calibrating turbulence quantities at the inlet to the diffuser (see also the discussion on the calibration of the numerical predictions in [4]). In order to better understand the effects of turbulence, turbulence measurements were performed with a single wire hotwire probe at various sections throughout the test rig and metal gauzes were inserted immediately downstream of the trailing edges of the preswirl vanes. This insertion of metal gauzes allowed modification of pressure and flow angle distributions in the diffuser and bend as well as the setting of different turbulence conditions in terms of intensity and length scale in the downstream sections. Another positive side effect of the inclusion of the metal gauzes is enhanced mixing of the wakes from the preswirl vanes. This leads to more uniform flow and a further reduction of clocking effects. Figure 13 shows pictures of preswirl vane trailing edges without (top) and with (bottom) metal gauze. The following results were obtained for the gauze shown in Fig. 13 which is composed of square bars (1mm thickness) with a separation distance of 4.8 mm from bar to bar. This yields a porosity of 62%.

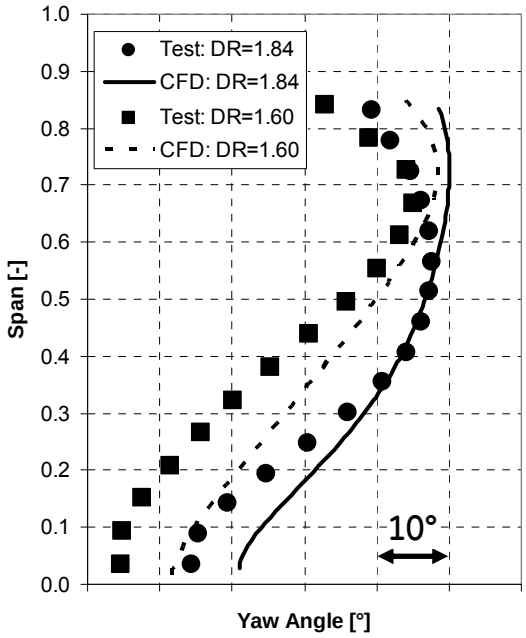

Figure 11: Circumferentially area averaged yaw angle as a function of span at the exit of the stage (section 4) at 98% design flow coefficient. Shown are measurements of predictions of two stators with diffusion ratios of 1.84 and 1.60.

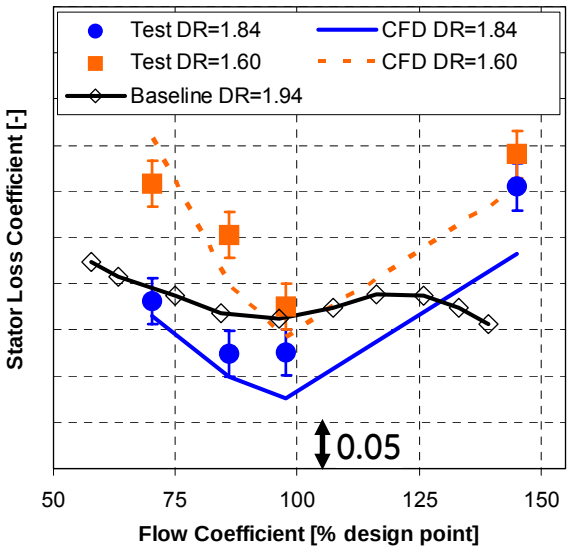

Figure 12: Stator loss coefficient as a function of flow coefficient. Shown are present measurements and predictions of two return channels with diffusion ratio 1.84 and 1.60 along with measurements of a rotating test with diffusion ratio 1.94.

One of the effects of introducing additional resistance at the inlet to the diffuser is a reduction in circumferential momentum that leads to smaller flow angles at section 2 and further downstream. This is illustrated in Fig. 14 which shows circumferentially area averaged yaw angle profiles at the inlet to the diffuser (section 2 of Fig. 2) that correspond to the 98% preswirl vanes with and without gauze. The average yaw angle obtained with the 62% porosity gauze is equivalent to an operating point of 129% of the design flow coefficient (as compared to 98% without gauze). Besides this shift, the profile is significantly more uniform in the spanwise direction. This is to illustrate that a careful selection of gauze porosity allows (within limits):

- investigating the sensitivity of return channel designs to different impeller exit conditions.
- shifting of the discrete operating points of fixed preswirl vane designs.

Careful selection of the dimensions of the gauze, such as the thickness of the bars and the separation distance between them, allows further adjustment of turbulence properties (intensity and length scale) at the entrance to the diffuser, Roach [14]. Figure 15 shows measured turbulence intensities (left) and calculated turbulence integral length scales [15] (right) at the inlet (section 2) and exit (section 3) of the diffuser for the 98% preswirl vanes with and without gauze. While the average turbulence intensity at the entrance to the diffuser remained relatively constant for both cases (nearly 10%), the turbulence length scale was significantly reduced by the gauze from approximately 6 mm down to 3 mm (the span height of the diffuser was 27 mm). The reduction in length scale implies an increase in turbulence dissipation. This is the reason the turbulence intensity at the exit of the diffuser is significantly smaller for the case of preswirl vanes with gauze as compared to preswirl vanes without gauze (9% vs. 13%). This can have considerable implications for the flow conditions in the 180° bend.

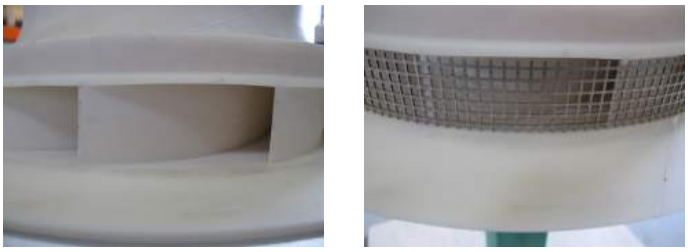

Figure 13: Picture of preswirl trailing edges without (left) and with (right) metal gauze.

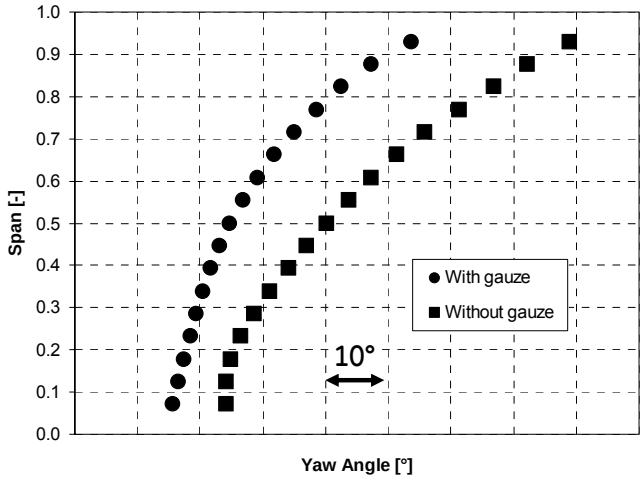

Figure 14: Circumferentially area averaged yaw angle as a function of span at the inlet to the diffuser (section 2) for the preswirl vanes corresponding to 98% design flow coefficient without gauze. Shown are the profiles without and with gauze.

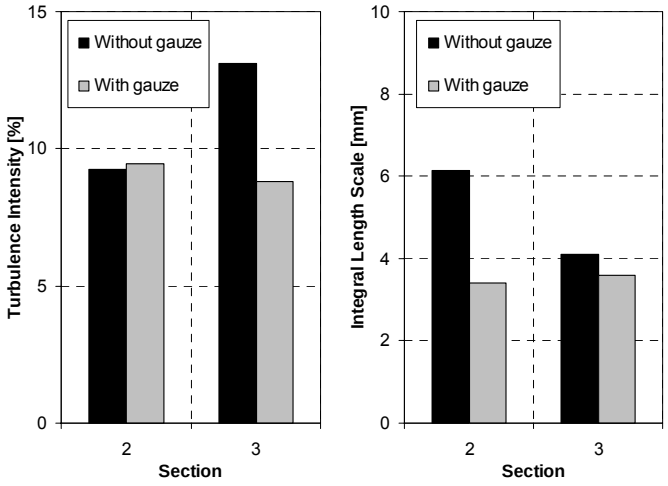

Figure 15: Measured turbulence intensity (left) and calculated integral length scale (right) at the inlet (section 2) and the exit (section 3) of the diffuser for the preswirl vanes corresponding to 98% design flow coefficient without and with gauze.

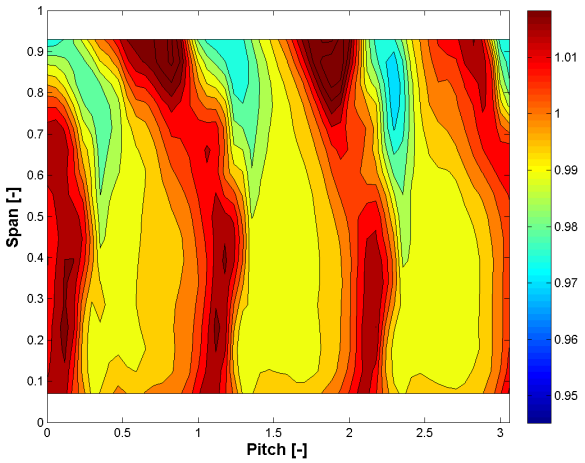

Figure 16: Contour plots of measured stagnation pressure at the inlet to the diffuser (section 2) for the preswirl vanes corresponding to 98% design flow coefficient with gauze. Pressures are normalized with the sectional average.

Finally, as mentioned in connection with the motivation for the additional investigation with the gauze, the presence of the gauze also reduces circumferential non-uniformities in the flow. Figure 16 shows contours of normalized stagnation pressure measured at the inlet to the diffuser (section 2) for the preswirl vanes corresponding to 98% design flow coefficient with gauze. The results correspond to Fig. 8 which shows measurements for the same condition, at the same scale, but without gauze. When comparing Fig. 16 with Fig. 8 it becomes clear that the strength of the wakes has been significantly reduced (it should be noted that the position of the wakes has been shifted due to different flow angles).

CONCLUSIONS

A full-annulus cascade for radial compressor stator development has been designed, commissioned and applied for the validation of new reduced radius designs. The cascade has further been used for an investigation into the effects of turbulence by means of inserting a gauze at the entrance to the diffuser. The main conclusions of the study are as follows:

1. The preswirl section of the full-annulus is capable of producing discrete operating points comparable to rotating impeller exit conditions except for the unsteadiness.
2. Overall measurement uncertainties for the stator loss coefficient were reasonable (11%) and sufficient for the purpose of screening different stator designs. Clocking effects between preswirl vanes and return channel vanes did not play a major role in the aero-response of the return channel.
3. Cascade results suggest that the diffusion ratio of a centrifugal compressor stage could be successfully reduced from 1.94 to 1.84 while also reducing losses across the majority of the operating characteristic.
4. The turnaround time from the design of a new geometry to its performance validation in the cascade was less than four weeks. The cost for validating the performance of a stator geometry in the cascade is approximately 20% of a full rotating test.
5. Numerical predictions of stator performance and flow details showed good qualitative and reasonable quantitative agreement with measurements.
6. Turbulence conditions, spanwise flow profiles and discrete operating points were successfully modified by inserting a gauze immediately downstream of the preswirl section.

ACKNOWLEDGMENTS

The authors would like to thank GE Oil&Gas for their support and also for granting permission to publish the results. The excellent work of H. Wehner-Stehlig in polishing and fitting the parts of the test rig together is also gratefully acknowledged.

REFERENCES

[1] Simpson, A., Aalburg, C., Schmitz, M., Pannekeet, R., Larisch, F., Michelassi, V., 2008, “Design, validation and application of a radial cascade for centrifugal compressors”, ASME GT2008-51262.
[2] Simpson, A., Aalburg, C., Schmitz, M., Pannekeet, R., Larisch, F., Michelassi, V., 2009, “Application of flow control in a novel sector test rig”, ASME GT2009-60126.
[3] Aalburg, C, Simpson, A., Carretero, J., Ngyuen, T., 2009, “Extension of the stator vane upstream across the 180º bend for a multistage radial compressor stage”, ASME GT2009-59522.
[4] Aalburg, C., Simpson, A. Schmitz, M.B., Michelassi, V., Evangelisti, S., Belardini, E., Ballarini, V., 2008, “Design and testing of multistage centrifugal compressors with small diffusion ratios”, ASME GT2008-51263.
[5] Howell, A.R., 1942, “The present basis of axial flow compressor design”, Aeronautical Research Council R and M 2095.
[6] Schmitz, M.B., Simpson, A., Aalburg, C., Michelassi, V., 2008, “Development of a sector test rig for multistage radial compressor stators“, ISROMAC12-2008-20254.
[7] Zwillinger, D., 1996, “CRC Standard Mathematical Tables and Formulae”, CRC Press, ISBN 0-8493-2479-3/96.
[8] Bearman, P., 1971, “Corrections for the effect of ambient temperature drift on hot wire measurements in incompressible flow”, DISA Information No. 11, pp. 25-30.
[9] Cumpsty, N.A., 1989, “Compressor Aerodynamics”, Longman Scientific and Technical, ISBN 0-582-01364-X, pp. 179-180.
[10] Schlichting, H., Das, A., 1969, “On the influence off turbulence level on the aerodynamic losses of axial

turbomachinery“, Proceedings of the symposium on flow research on blading.
[11] de Haller, P., 1953, “Das Verhalten von Tragfluegelgittern in Axialverdichtern und in Windkanal“, Brennstoff-Waerme-Kraft 5, Heft 10.
[12] Wisler, D.C., Bauer, R.C., Okiishi, T.H., 1987, “Secondary flow, turbulent diffusion and mixing in axial-flow compressors, Trans ASME Journal of Turbomachinery 109: 455-82.
[13] Japikse, D., Baines, N.C., 1998, “Diffuser Design Technology”, Concepts ETI, ISBN 0-933283-08-3.
[14] Roach, P.E., 1986, “The generation of nearly isotropic turbulence by means of grids”, Journal of Heat and Flow, 8(2), pp. 82-92.
[15] Schlichting, H., Gersten, K., 2000, “Boundary Layer Theory”, Chapter 6.